Centimeter continuum observations of the northern head of the HH 80/81/80N jet: revising the actual dimensions of a parsec scale jet

Josep M. Masqué[1], Josep M. Girart[2], Robert Estalella[1], Luis F. Rodríguez[3]

and

Maria T. Beltrán[4]

ABSTRACT

We present 6 and 20 cm JVLA/VLA observations of the northern head of the HH 80/81/80N jet, one of the largest collimated jet systems known so far, aimed to look for knots further away than HH 80N, the northern head of the jet. Aligned with the jet and 10′ northeast of HH 80N, we found a radio source not reported before, with a negative spectral index similar to that HH 80, HH 81 and HH 80N. The fit of a precessing jet model to the knots of the HH 80/81/80N jet, including the new source, shows that the position of this source is close to the jet path resulting from the modeling. If the new source belongs to the HH 80/81/80N jet, its derived size and dynamical age are 18.4 pc and $> 9 \times 10^3$ yr, respectively. If the jet is symmetric, its southern lobe would expand beyond the cloud edge resulting in an asymmetric appearance of the jet. Based on the updated dynamical age, we speculate on the possibility that the HH 80/81/80N jet triggered the star formation observed in a dense core found ahead of HH 80N, which shows signposts of interaction with the jet. These results indicate that pc scale radio jets can play a role on the stability of dense clumps and the regulation of star formation in the molecular cloud.

[1]Departament d'Astronomia i Meteorologia, Universitat de Barcelona, Martí i Franquès 1, 08028 Barcelona, Catalunya, Spain

[2]Institut de Ciències de l'Espai, (CSIC-IEEC), Campus UAB, Facultat de Ciències, Torre C5 - parell 2, 08193 Bellaterra, Catalunya, Spain

[3]Centro de Radioastronomía y Astrofísica, Universidad Nacional Autónoma de México, Apartado Postal 3-72, 58090 Morelia, Michoacán, México

[4]INAF - Osservatorio Astrofisico di Arcetri, Largo E. Fermi 5, 50125 Firenze, Italy

1. Introduction

Expanding Herbig-Haro (HH) flows arising from protostellar objects are among the most spectacular observed phenomena during the star formation process (Herbig & Jones 1981). HH flows, which can extend over parsec scale distances (Poetzel et al. 1989), are signposts of interaction of the protostellar activity with the ambient cloud medium. At scales of a fraction of parsec from the powering protostar, they appear collimated showing a jet-like morphology (Mundt et al. 1987). However, at parsec scales the collimation is less evident because first, the possible precession can enhance an S-shaped morphology for the flow and, second, the common presence of multiple outflow sources in star forming clouds may cause contamination by neighboring flows (Bally & Devine 1994; Reipurth et al. 1997). As a consequence, the measurement of the actual length of HH flows can be sometimes controversial, since it is not easy to associate distant and tentative HH objects to a specific HH flow without further evidence (e.g. through proper motions or physical properties of the object).

A peculiar case, the HH 80/81/80N jet, is found in the region GGD 27 (Gyulbudaghian et al. 1978), located in Sagittarius at a distance of 1.7 kpc (Rodríguez et al. 1980). The jet is powered by a young, high-luminosity protostellar object, IRAS 18162−2048 with a total luminosity of 1.7×10^4 $L_\odot$, derived from the IRAS survey. Recently, Fernández-López et al. (2011a,b) detect compact millimeter emission towards this source, which is interpreted by these authors as arising from a massive (~ 4 $M_\odot$), and compact ($r \lesssim 300$ AU) disk. VLA observations carried out towards IRAS 18162−2048 by Rodríguez & Reipurth (1989) reveal that this source is elongated, pointing to the south toward HH 80 and 81, the brightest Herbig-Haro objects known. HH 80N is located 3 pc north of IRAS 18162−2048 and is the northern counterpart of HH 80 and 81. HH 80N has only been detected at radio wavelengths due to the possible high extinction of this region (Martí et al. 1993). These authors have also found several radio knots aligned with the central source and the HH objects, which indicates that these condensations probably trace a highly collimated jet. Evidence of wiggling of the flow axis suggests that the driving source is precessing, and preserving the collimation up to scales of ~ 5 pc, being one of the largest collimated jet systems known so far (Martí et al. 1993). The high outflow velocities of 500 km s^{-1}, derived from proper motions measurements (Martí et al. 1995, 1998), suggest that the emission arising from the radio jet is due to very strong shocks (Heathcote et al. 1998). Synchrotron radiation, indicating the presence of relativistic electrons, has been recently found in this jet (Carrasco-González et al. 2010).

In this letter we report the results of recent cm continuum observations carried out with the Jansky Very Large Array (JVLA)/Very Large Array (VLA) toward the northern lobe of the HH 80/81/80N jet aimed at looking for knots further away than HH 80N. Up to date, HH 80N is assumed to be the head of the HH 80/81/80N jet. Determining the true size and

age of the jet is crucial, as it can be an important supplier of energy and momentum to the cloud. Therefore, the HH 80/81/80N jet is a good target to investigate the effects of pc scale jets on star formation in molecular clouds.

2. Observations and results

JVLA/VLA continuum observations of the northern part of the HH 80/81/80N radio-jet were carried out on June 2009 in the C configuration (6 and 20 cm bands) and October 2009 in the D configuration (6 cm band). The phase center was always set at the position of the HH 80N object, $\alpha(J2000) = 18^{\rm h}19^{\rm m}19\overset{\rm s}{.}74$ and $\delta(J2000) = -20°41'34\overset{''}{.}9$, except for the D configuration observations, for which we performed a two point mosaic with one field centered on the HH 80N position and the other offset (81″, 328″). A bandwidth of 100 MHz (for the two polarizations) was employed. The flux calibrator was always 3C286 and the phase calibrators were J1820−254 at 6 cm and J1833−210 at 20 cm. The data were edited and calibrated using the AIPS package of NRAO.

The maps were highly contaminated by the emission of a strong radio source, J1819−2036, located at $\alpha(J2000) = 18^{\rm h}19^{\rm m}36\overset{\rm s}{.}9$ and $\delta(J2000) = -20°36'31\overset{''}{.}0$. This source was first reported by Furst et al. (1990) from a radio continuum survey at 11 cm obtained with the Effelsberg 100m antenna (their source num. 359). The flux density measured in our 6 and 20 cm maps is 113.0 ± 0.3 and 202.5 ± 0.2 mJy, respectively. In order to avoid the strong sidelobes generated by this source, its clean components were subtracted from the visibility dataset of each block. The resulting final maps of the GGD 27 region are shown in Figure 1.

Figure 1 shows that IRAS 18162−2048 is elongated, pointing to HH 80N. A few marginal knots appear in the map connecting both objects following the shape of a jet. This is best seen in the 6 cm map obtained with the D configuration. The 6 cm map in the C configuration proves that the jet is very well collimated. At 20 cm, contamination at short baselines, probably due to Galactic background emission, prevented the proper imaging of the extended emission.

Table 1 gives the measured position, flux at 6 and 20 cm, and the spectral index of the sources belonging to the HH 80/81/80N radio-jet. Our flux values are systematically slightly lower than those reported in Table 2 of Martí et al. (1993), possibly due to calibration uncertainties. The spectral indices are consistent with those derived by Martí et al. (1993) except for HH 80N, for which we found a spectral index slightly more negative. All spectral indices are well below the minimum value required for having free-free emission (-0.1, Rodríguez et al. 1993), which suggests that the contribution of synchrotron emission

is significant (Carrasco-González et al. 2010). Source 33 has very negative spectral index (~ -0.8). This source is not aligned with the jet path and is likely extragalactic.

Source 34, detected at the 6 and 20 cm bands with no associated counterparts at any other wavelength, appears to be located about $6'$ north of HH 80N ($\sim 10'$ from IRAS 18162-2048), roughly in the direction of the HH 80/81/80N radio jet. This source, not reported before, has a negative spectral index of -0.46, similar to the values found for HH 80, HH 81 and HH 80N, and characteristic of the jet. The D configuration map at 6 cm (Fig. 1) shows that this source is elongated in the north-south direction aligned roughly with the direction of the jet. What is the a priori probability that Source 34 is a background source unrelated to the star forming region? We will assume that we would have considered the source associated with the outflow if it appeared anywhere inside a rectangular box with dimensions of $0\farcm5 \times 10'$ with its major dimension along the outflow axis. The solid angle of this rectangle is 5 square arcmin. Following Fomalont et al. (1991) the a priori probability of finding a 1 mJy background source at 6 cm inside such a solid angle is only $\sim$0.03. We then consider unlikely that Source 34 is not associated with the star forming region.

Martí et al. (1993) found that the different radio knots of the HH 80/81/80N radio jet are not completely aligned but rather follow locations compatible with a precessing jet. In order to test if Source 34 is part of the HH 80/81/80N jet, we extrapolated the expected path of the jet modeled by Martí et al. (1993) assuming that the jet is precessing with the jet axis in the plane of sky. Using the coordinates (x, y), with y perpendicular to the jet axis and x along the jet axis, the y position of a knot is given by the sinusoidal expression.

$$y = x \tan(\beta) \cos(\varphi_p - 2\pi \frac{|x|}{\lambda_p}) \quad (1)$$

where β is the half-opening angle of the jet, φ_p is the initial precession phase angle for $x = 0$, and λ_p is the wavelength of the wiggles in the plane of sky.

Table 2 gives the results of the fit of the expression (1) to the knots of the HH 80/81/80N jet, without including Source 34 (i.e. aimed at reproducing the results of Martí et al. (1993), model A) and including this source (model B). In this analysis we also employed Martí et al. (1993) data obtained from observations in the C configuration at 6 cm, which have a field of view covering the jet from HH 80N to HH 80/81, in order to include Source 13, HH 81 and HH 80. The resulting sinusoidal path for both models are shown in Figure 2. This figure shows the map resulting from the observations reported in Martí et al. (1993) combined with the new data reported in this letter obtained in the C configuration at 6 cm. The parameters of Model A have values similar to those obtained in Martí et al. (1993) as expected (note that the precession angle in Martí et al. (1993) is the full opening angle, i.e. 2β). However,

the sinusoidal path resulting from this fit misses Source 34 by about 20″ (see blue line of Fig. 2). On the other hand, model B yields a jet path close to Source 34 (see red line of Fig. 2). The parameters of both models have similar values except for φ_p and λ_p. As seen in Fig. 2, in the model B, the jet has longer wiggles in the plane of the sky with respect to model A.

3. Discussion

Given the symmetry of the HH 80/81/80N radio knots, it is plausible that Source 34 has a counterpart in the southern lobe. We inspected the 20 cm map but did not detect any emission above 1.6 mJy at the expected counterpart position. Note that this is not a stringent upper limit due to the contamination at low baselines caused probably by galactic extended emission. We also checked surveys observed at wavelengths suited to detect HH shock emission (e.g. Hα SuperCosmos) but found no emission around the expected counterpart position. Also, this position falls outside the field of view of the 6 cm band observations. Nevertheless, observations of HH complexes show that they are not necessarily strictly symmetric (HH 111: Rodriguez & Reipurth 1994; HH 34: Stapelfeldt et al. 1991; Anglada et al. 1995). The asymmetry of the HH 80/81/80N jet could be caused by the fact that the southern lobe of the jet moves beyond the edge of the cloud, changing the flow appearance further away than HH 80 because it enters in a low pressure medium. The projected distance from HH 80N to the southern bow shock beyond HH 80 at a distance of 1.7 kpc is 7.5 pc (Heathcote et al. 1998). If Source 34 belongs to the HH 80/81/80N jet then its total extent to the plane of sky is 10.3 pc. Correcting from inclination effects using 56° for the value of the angle of the jet axis to the plane of the sky (Heathcote et al. 1998), we derive 18.4 pc of total extent of the HH system. This updated size is 5.0 pc larger than the size previously stablished by Heathcote et al. (1998).

The extraordinary collimation of the HH 80/81/80N jet extending from the new reported Source 34 to HH 80 and 81 is in agreement with the idea that the ejection mechanism of the jet operates similarly as in the low luminosity protostars. However, the results presented here show that the collimation and symmetry of pc scale jets tend to break at some point because the chances of finding a heterogeneous medium are higher as the jet propagates far away in the cloud. IRAS 18162−2048 also reveals similarities with low luminosity protostars. Continuum mm observations towards this source suggest that the emission arises from a massive and compact disk surrounding the driving source of the HH 80/81/80N jet (Fernández-López et al. 2011a; Carrasco-González et al. 2012). The derived mass ratio between the disk and the central star is $\lesssim 0.3$ (Carrasco-González et al. 2012), which seems to be consistent with the

typical values found for low mass protostars. These authors also obtained a crude estimate for the mass accretion rate of the disk onto the central powering protostar of 10^{-4} $M_{\odot}$ yr^{-1}. Adopting a mass for the central object of $7 - 11$ $M_{\odot}$ (Fernández-López et al. 2011b), the accretion phase must have started between $(0.7 - 1.1) \times 10^5$ yr ago.

Assuming that HH 80N is the northern end of the HH 80/81/80N jet and all its condensations move ballistically with a constant spatial velocity of 625 km s^{-1} (obtained using the average tangential velocity of HH 80 and HH 81 and the angle of the jet axis to the plane of sky of Heathcote et al. 1998), we derive a dynamical age of $\sim 5 \times 10^3$ yr for the jet. However, if Source 34 belongs to the HH 80/81/80N jet, the dynamical age increases to $\sim 9 \times 10^3$ yr. Furthermore, the HH 80/81/80N jet may be decelerating as a consequence of the loss of kinetic energy as the jet passes through the cloud, as indicated by the high mechanical luminosity of HH 80N (a few 10^1 $L_{\odot}$, Girart et al. 1994). For this case, the dynamical age must be $> 9 \times 10^3$ yr, consistent with the upper limit for the age of the accretion phase of IRAS 18162−2048 derived above.

Ahead of HH 80N there is a dense core extensively studied by our team with signatures of star formation and supersonic infall velocities (Girart et al. 1994, 1998, 2001; Masqué et al. 2009, 2011). Given the close location of the core to the most powerful jet known and its peculiar kinematics, it has been suggested that the star formation of this core has been triggered or at least sped up by the HH 80/81/80N jet (Girart et al. 2001; Masqué et al. 2011). The estimated age of the protostar embedded in the HH 80N core (2×10^4 yr, Masqué et al. 2011) falls in the range comprised between the lower limit of the estimated dynamical age of the jet and the upper limit of the age of the main accretion phase of its energy source, $(0.9 - 11.0) \times 10^4$ yr. Moreover, our observations of high density tracers in the HH 80N region (Masqué et al. 2012, in prep.) suggest that there is a dynamical interaction between HH 80/81/80N jet and the HH 80N core: the velocity gradients of the high density gas are consistent with the possibility that part of the core is being swept by the HH 80/81/80N jet in the process of dissipating energy. This could turn some regions in the core gravitationally unstable. This possibility appears also evident in the high angular resolution continuum maps of the HH 80N core (Masqué et al. 2011), which show that the HH 80N core is fragmenting into several condensations, one of them clearly associated with the embedded object in the core. Therefore, the HH 80/81/80N jet may play a role in the star formation process of the HH 80N core. Conclusive evidence for this possibility would provide an illustrative case of sequential star formation in a cloud occurring at scales of parsecs.

JMM, JMG and RE are supported by the Spanish MINECO AYA2011-30228-C03 and the Catalan AGAUR 2009SGR1172 grants.

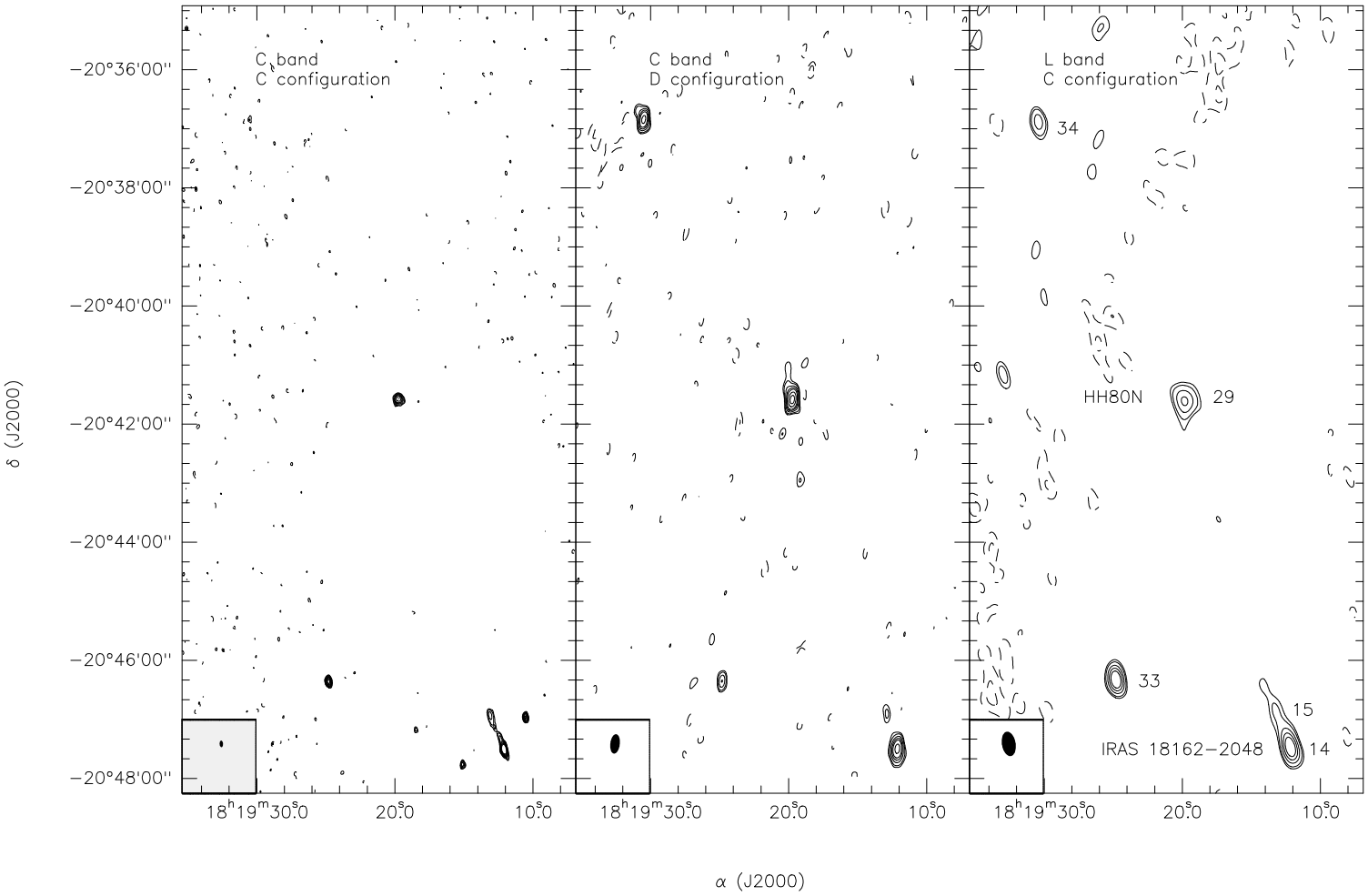

Fig. 1.— Northern lobe of the HH 80/81/80N jet mapped with centimeter continuum emission. The left panel shows the 6 cm continuum map obtained with C configuration. The center panel shows the 6 cm continuum map obtained with D configuration. The right panel shows the 20 cm continuum map obtained with C configuration. Contour levels are -3, 3, 4, 6, 8, 10, 14, 18, and 25 times 40, 65 and 250 μJy, the rms noise of the left, middle and right maps, respectively. The beam is shown in the bottom left corner of each panel: $6.6'' \times 3.5''$ and P.A. of -2.7° (*left panel*), $19.9'' \times 9.7''$ and P.A. of 10.0° (*center panel*), and $25.1'' \times 14.0''$ and P.A. of -2.9° (*right panel*). The numbers on the right panel label the sources found in the field following the Martí et al. (1993) nomenclature.

Table 1: Parameters of the knots of the HH 80/81/80N jet[a]

	Peak Position		$S_{20\mathrm{cm}}$	$S_{6\mathrm{cm}}$	
Source	α (J2000)	δ (J2000)	(mJy)	(mJy)	Spectral Index
7[b,c,d]	$18^{\mathrm{h}}19^{\mathrm{m}}06\overset{\mathrm{s}}{.}122$	$-20°51'49\overset{''}{.}486$	16.83 ± 0.07[e]	0.77 ± 0.06	≥ -2.47
8[b,c,f]	$18^{\mathrm{h}}19^{\mathrm{m}}06\overset{\mathrm{s}}{.}652$	$-20°51'05\overset{''}{.}822$	”	1.54 ± 0.07	≥ -1.91
13[c]	$18^{\mathrm{h}}19^{\mathrm{m}}10\overset{\mathrm{s}}{.}554$	$-20°48'29\overset{''}{.}239$	0.69 ± 0.06	0.52 ± 0.10	-0.22 ± 0.17
14[g]	$18^{\mathrm{h}}19^{\mathrm{m}}12\overset{\mathrm{s}}{.}106$	$-20°47'30\overset{''}{.}834$	3.77 ± 0.10	4.29 ± 0.06	0.11 ± 0.01
15[b,c]	$18^{\mathrm{h}}19^{\mathrm{m}}13\overset{\mathrm{s}}{.}086$	$-20°46'55\overset{''}{.}713$	1.09 ± 0.07	1.06 ± 0.10	-0.02 ± 0.09
29[h]	$18^{\mathrm{h}}19^{\mathrm{m}}19\overset{\mathrm{s}}{.}780$	$-20°41'33\overset{''}{.}343$	3.72 ± 0.20	2.05 ± 0.15	-0.49 ± 0.04
34[i]	$18^{\mathrm{h}}19^{\mathrm{m}}30\overset{\mathrm{s}}{.}489$	$-20°36'51\overset{''}{.}315$	1.82 ± 0.05	1.03 ± 0.03	-0.46 ± 0.02

Notes.

[a]Derived from a Gaussian fit

[b]Sources with position outside the field of view of Fig. 1

[c]6 cm fluxes were obtained using Martí et al. (1993) data at C configuration

[d]HH 80

[e]Sources 7 and 8 appear blended in the 20 cm map

[f]HH 81

[g]IRAS $18162-2048$

[h]HH 80N

[i]New reported source

Table 2: Fit results of a precessing jet to the knots of the HH 80/81/80N radio jet

	Rms fit residual	β	λ_p	ψ	φ_p
Model	(arcsec)	(deg)	(arcsec)	(deg)	(rad)
A	3.5	2.7 ± 0.4	470 ± 30	19.5 ± 0.3	4.9 ± 0.4
B	3.2	2.7 ± 0.5	620 ± 40	19.4 ± 0.4	4.2 ± 0.3

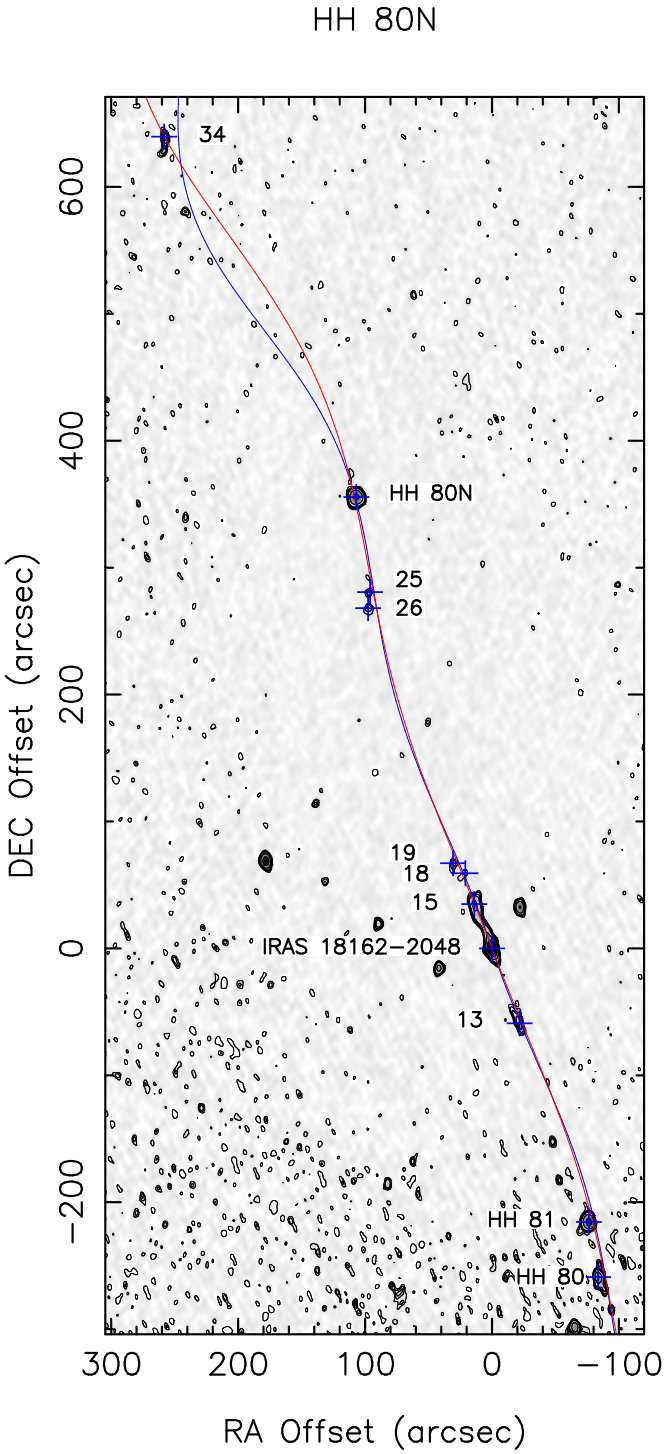

Fig. 2.— Fit of a precessing jet to the knots of the HH 80/81/80N complex (blue crosses) plotted over the 6 cm map obtained with the C configuration (including Martí et al. (1993) data) convolved with a Gaussian of 15″ of FHWM. The numbers follow the Martí et al. (1993) nomenclature and indicate the knots used in the fit of a precessing jet (see text). The blue solid line shows the precessing jet path obtained using the parameters of model A (without including Source 34) while the red solid line shows the resulting jet path using the parameters of model B (including Source 34). The reference position of the map is located at IRAS 18162−2048.

REFERENCES

Anglada, G., Estalella, R., Mauersberger, R., et al. 1995, ApJ, 443, 682

Bally, J., & Devine, D. 1994, ApJ, 428, L65

Carrasco-González, C., Rodríguez, L. F., Anglada, G., et al. 2010, Science, 330, 1209

Carrasco-González, C., Galván-Madrid, R., Anglada, G., et al. 2012, ApJ, 752, L29

Fernández-López, M., Curiel, S., Girart, J. M., et al. 2011a, AJ, 141, 72

Fernández-López, M., Girart, J. M., Curiel, S., et al. 2011b, AJ, 142, 97

Fomalont, E. B., Windhorst, R. A., Kristian, J. A., & Kellerman, K. I. 1991, AJ, 102, 1258

Furst, E., Reich, W., Reich, P., & Reif, K. 1990, A&AS, 85, 805

Girart, J., Estalella, R., & Ho, P. T. P. 1998, ApJ, 495, L59+

Girart, J. M., Estalella, R., Viti, S., Williams, D. A., & Ho, P. T. P. 2001, ApJ, 562, L91

Girart, J. M., Rodríguez, L. F., Anglada, G., et al. 1994, ApJ, 435, L145

Gyulbudaghian, A. L., Glushkov, Y. I., & Denisyuk, E. K. 1978, ApJ, 224, L137+

Heathcote, S., Reipurth, B., & Raga, A. C. 1998, AJ, 116, 1940

Herbig, G. H., & Jones, B. F. 1981, AJ, 86, 1232

Martí, J., Rodríguez, L. F., & Reipurth, B. 1993, ApJ, 416, 208

—. 1995, ApJ, 449, 184

—. 1998, ApJ, 502, 337

Masqué, J. M., Girart, J. M., Beltrán, M. T., Estalella, R., & Viti, S. 2009, ApJ, 695, 1505

Masqué, J. M., Osorio, M., Girart, J. M., et al. 2011, ApJ, 738, 43

Mundt, R., Brugel, E. W., & Buehrke, T. 1987, ApJ, 319, 275

Poetzel, R., Mundt, R., & Ray, T. P. 1989, A&A, 224, L13

Reipurth, B., Bally, J., & Devine, D. 1997, AJ, 114, 2708

Rodríguez, L. F., Moran, J. M., Ho, P. T. P., & Gottlieb, E. W. 1980, ApJ, 235, 845

Rodríguez, L. F., & Reipurth, B. 1989, Rev. Mexicana Astron. Astrofis., 17, 59

Rodríguez, L. F., Marti, J., Canto, J., Moran, J. M., & Curiel, S. 1993, Rev. Mexicana Astron. Astrofis., 25, 23

Rodriguez, L. F., & Reipurth, B. 1994, A&A, 281, 882

Stapelfeldt, K. R., Scoville, N. Z., Beichman, C. A., Hester, J. J., & Gautier, III, T. N. 1991, ApJ, 371, 226